Article

Abiotic Metallofoldamers as Electrochemically Responsive Molecules

Fan Zhang, Shi Bai, Glenn P. A. Yap, Vinod Tarwade, and Joseph M. Fox

J. Am. Chem. Soc., **2005**, 127 (30), 10590-10599• DOI: 10.1021/ja050886c • Publication Date (Web): 12 July 2005

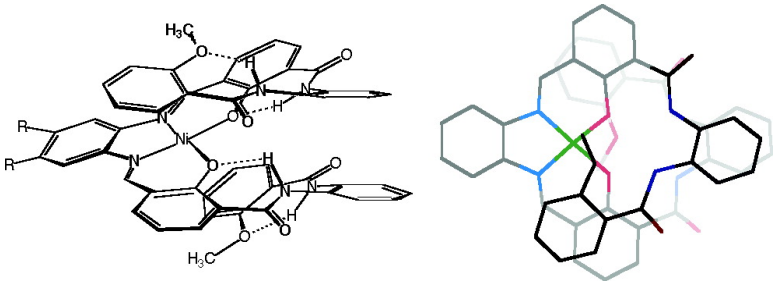

More About This Article

J|A|C|S
ARTICLES
Published on Web 07/12/2005

Abiotic Metallofoldamers as Electrochemically Responsive Molecules

Fan Zhang, Shi Bai,† Glenn P. A. Yap,† Vinod Tarwade, and Joseph M. Fox*

Contribution from the Brown Laboratories, Department of Chemistry and Biochemistry, University of Delaware, Newark, Delaware 19716

Received February 10, 2005; E-mail: jmfox@udel.edu

Abstract: Described are the design, synthesis, and study of nonbiological molecules based on salophen and salen ligands that fold into single-stranded helices in the presence of either Ni(II) or Cu(II). X-ray diffraction studies show that the materials fold into helical structures in the solid state, and a series of NMR studies provide strong evidence that the folded structures are conserved in solution. Metal coordination is required for folding, as NMR and X-ray show that the free ligands do not adopt helical structures. Two of the racemic metallofoldamers spontaneously resolve during crystallization from $CHCl_3$/acetonitrile, and CD spectroscopy and optical rotation show that the resolved, crystalline materials racemize quickly when dissolved at 5 °C. This shows that the secondary structures can reorganize easily and can, therefore, provide the basis for responsive materials. By comparison, an analogue from enantiomerically pure (*R,R*)-(−)-*trans*-cyclohexanediamine showed a strong CD signal and a large specific rotation. Electrochemical experiments show that a structural reorganization occurs upon metal-centered reduction of a Cu(II)-containing foldamer. When the reduction is carried out in the presence of coordinating ligands, it is proposed that apical binding of those ligands gives square pyramidal complexes. Semiempirical (AM1) calculations support that the helical structure would be disrupted by the reduction to Cu(I) with concomitant reorganization to a square pyramidal complex.

Introduction

In this contribution, we describe the synthesis and characterization of single-stranded abiotic foldamers[1−3] that adopt helical conformations in response to metal complexation. These metallofoldamers are derivatives of salen and salophen ligands—frameworks that are well established in diverse fields, such as enantioselective catalysis,[4] liquid crystals,[5,6] and nonlinear optical materials.[7,8] Electrochemistry can be used to reversibly alter the coordination environment for one of the metallofoldamers, with the implicit consequence that the entire secondary structure is altered, as well. This provides a basis for correlating the aforementioned materials' properties to electrochemistry and other types of external switching mechanisms (e.g., photochemistry) that can alter metal geometry. The concept is illustrated in Scheme 1.

Scheme 1

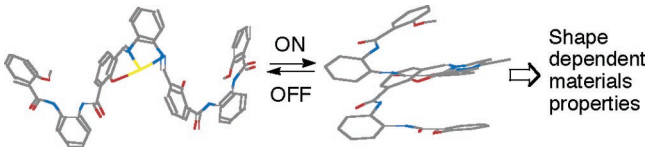

The interplay between metal geometry, secondary structure, and function is well established in biology and has, consequently, served as the inspiration for the design of "foldamers"[1,2]—unnatural molecules that fold into compact secondary structures. Foldamers have been broadly classified as mimics of peptides[1,2,9] and oligonucleotides[10] and the abiotic analogues of each.[11,12]

† Questions regarding NMR and X-ray should be addressed to Dr. Bai (bais@udel.edu) and Dr.Yap (gpyap@chem.udel.edu), respectively.

(1) Gellman, S. H. *Acc. Chem. Res.* **1998**, *31*, 173−180.
(2) (a) Hill, D. J.; Mio, M. J.; Prince, R. B.; Hughes, T. S.; Moore, J. S. *Chem. Rev.* **2001**, *101*, 3893−4012.
(3) We use Moore's system of nomenclature to distinguish peptidomimetic foldamers from their abiotic analogues. Paraphrasing from pages 3910 and 3944 of ref 2: peptidomimetic foldamer research is defined as a 'top-down' design approach that involves structural variations of parent chain molecules known to undergo folding reactions. Research on their abiotic analogues employs a 'bottom-up' design approach, where analogous architectures to biomacromolecules are obtained by backbones that bear little resemblance to natural chains.
(4) Larrow, J. F.; Jacobsen, E. N. *Top. Organomet. Chem.* **2004**, *6*, 123−152.
(5) Lead references to liquid crystalline Salen metal complexes: (a) Abe, Y.; Nakabayashi, K.; Matsukawa, N.; Iida, M.; Tanese, T.; Sugibayashia, M.; Ohta, K. *Inorg. Chem. Commun.* **2004**, *7*, 580−583. (b) Paschke, R.; Balkow, D.; Sinn, E. *Inorg. Chem.* **2002**, *41*, 1949−1953. (c) Miyamura, K.; Mihara, A.; Fujii, T.; Gohshi, Y.; Ishii, Y. *J. Am. Chem. Soc.* **1995**, *117*, 2377−2378. (d) Serrette, A.; Carroll, P. J.; Swager, T. M. *J. Am. Chem. Soc.* **1992**, *114*, 1887−1889.
(6) For materials that can switch liquid crystalline materials: Feringa, B. L.; van Delden, R. A.; Koumura, N.; Geertsema, E. M. *Chem. Rev.* **2000**, *100*, 1789−1816.
(7) Di Bella, S. *Chem. Soc. Rev.* **2001**, *30*, 355−366.
(8) For materials whose NLO properties can be switched by electrochemistry: (a) Powell, C. E.; Humphrey, M. G.; Cifuentes, M. P.; Morrall, J. P.; Samoc, M.; Luther-Davies, B. *J. Phys. Chem. A* **2003**, *107*, 11264−11266 and references therein. For a review that covers photoswitchable NLO materials: (b) Delaire, J. A.; Nakatani, K. *Chem. Rev.* **2000**, *100*, 1817−1846.
(9) Reviews and lead references to peptidomimetics: (a) Porter, E. A.; Wang, X.; Lee, H.-S.; Weisblum, B.; Gellman, S. H. *Nature* **2000**, *404*, 565. (b) Seebach, D.; Matthews, J. L. *J. Chem. Soc., Chem. Commun.* **1997**, 2015−2022. (c) Degrado, W. F.; Schneider, J. P.; Hamuro, Y. *J. Peptide Res.* **1999**, *54*, 206−217. (d) Kirshenbaum, K.; Zuckermann, R. N.; Dill, K. A. *Curr. Opin. Struct. Biol.* **1999**, *9*, 530−535. (e) Stigers, K. D.; Soth, M. J.; Nowick, J. S. *Curr. Opin. Chem. Biol*. **1999**, *3*, 714−723.
(10) Reviews and lead references to oligonucleotide mimetics: (a) Eschenmoser, A.; Loewenthal, E. *Chem. Soc. Rev.* **1992**, *21*, 1−16. (b) Herdewijn, P. *Biochim. Biophys. Acta* **1999**, *1489*, 167−179. (c) Nielsen, P. E.; Haaima, G. *Chem. Soc. Rev.* **1997**, *26*, 73−78.

10.1021/ja050886c CCC: $30.25

Scheme 2

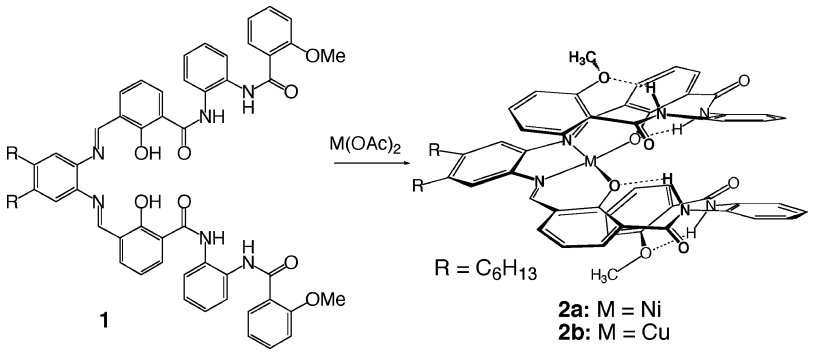

Mimics of oligonucleotides that bind metals are well-known for abiotic systems,[11] but analogues of peptides are rare[12,13] and consist mainly of molecules in which the metal serves as a *template* for a helical secondary structure. Thus, most abiotic mimics of metallopeptides bear analogy to the structure in Figure 1a,[13d] in which the metal coordination sphere is inherently helical.[13] In contrast, we are not aware of abiotic materials of the type outlined in Figure 1b, in which metal coordination *nucleates* the formation of a nonbiological single-stranded helix. That is, the metal coordination sphere is not inherently chiral, but instead causes a series of cooperative, noncovalent interactions that ultimately result in a folded structure. The closest precedent of such a material has been described by Moore, in which an oligophenyleneethynylene with radially oriented nitrile ligands binds two separate silver atoms.[13] That material can be considered to be a hybrid of the extremes in Figure 1.[14] Another related material has been reported by Lee and co-workers, in which the metal is a structural unit of the backbone of a single-stranded abiotic foldamer.[13f] On the basis of small-angle X-ray data, it was proposed that the secondary structure could be altered by varying the counterion of the metal.[13f]

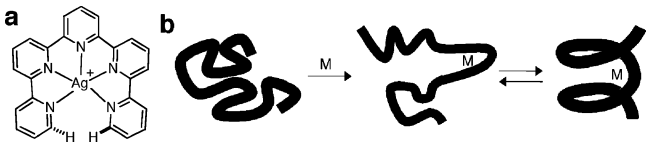

Figure 1. Classification of abiotic analogues of metallopeptides as (a) templated and (b) nucleated secondary structures.

In this contribution, we show that Ni(II) and Cu(II) complexes **2a** and **2b**, unlike the free ligand **1**, adopt well-defined helical structures in the crystalline state and in solution (Scheme 2). Remarkably, both **2a** and **2b** undergo dynamic resolution (to >94% ee) upon crystallization; crystal growth experiments produced a single crystal that racemizes immediately when redissolved at 5 °C. Despite their rapid racemization, a single conformation is observed by NMR, and NOE shows that the structure is very similar to that of the crystal. Thus, **2a** and **2b** are fluxional molecules in solution whose thermodynamically most favored conformations are helical. Smaller analogues of **1** have also been characterized crystallographically and by NMR spectroscopy. Their Ni complexes are also helical, but the free ligands are not. Cyclic voltamograms and modeling experiments show that electrochemical reduction of **2b** in a coordinating environment is followed by a change in the coordination geometry at the metal center that consequently alters the secondary structure of the entire molecule. Salen and salophen metal complexes have been applied in diverse areas of materials science, and the incorporation of salen and salophen structures into chiral polymers is known to produce materials with exceptional chiroptical properties.[15−17] For complexes such as **2b**, the chiral order in the folded state should correlate to useful properties (e.g., 2nd order NLO; induction of chiral nematic liquid crystalline phases) that can be switched on/off by folding/unfolding. Toward such applications, this work shows that electrochemistry can be used to reversibly switch the structure of Cu complex **2b** from a thermodynamically helical state [as tetracoordinate Cu(II)] to a nonhelical state [as pentacoordinate Cu(I)].

Results and Discussion

Design and Synthesis. The rationale for salen and salophen metal complexes that form single-stranded helical foldamers is

(11) Reviews and lead references to abiotic single-stranded foldamers: (a) Moore, J. S. *Acc. Chem. Res.* **1997**, *30*, 402−413. (b) Gin, M. S.; Yokozawa, T.; Prince, R. B.; Moore, J. S. *J. Am. Chem. Soc.* **1999**, *121*, 2643−2644. (c) Stone, M. T.; Fox, J. M.; Moore, J. S. *Org. Lett.* **2004**, *6*, 3317−3320. (d) Hamuro, Y.; Geib, S. J.; Hamilton, A. D. *J. Am. Chem. Soc.* **1997**, *119*, 10587−15093. (e) Hamuro, Y.; Hamilton, A. D. *Bioorg. Med. Chem.* **2001**, *9*, 2355−2363. (f) Gong, B. *Chem.—Eur. J.* **2001**, *7*, 4336−4342. (g) Yang, X.; Yuan, L.; Yamato, K.; Brown, A. L.; Feng, W.; Furukawa, M.; Zeng, X. C.; Gong, B. *J. Am. Chem. Soc.* **2004**, *126*, 3148−3162. (h) Huc, I. *Eur. J. Org. Chem.* **2004**, 17−29. (i) Jiang, H.; Dolain, C.; Leger, J.-M.; Gornitzka, H.; Huc, I. *J. Am. Chem. Soc.* **2004**, *126*, 1034−1035. (j) Zych, A. J.; Iverson, B. L. *J. Am. Chem. Soc.* **2000**, *122*, 8898−8909. (k) Berl, V.; Huc, I.; Khoury, R. G.; Lehn, J. M. *Chem.—Eur. J.* **2001**, *7*, 2798−2809. (l) Cuccia, L. A.; Lehn, J.-M.; Homo, J.-C.; Schmutz, M. *Angew. Chem., Int. Ed.* **2000**, *39*, 233−237. (m) Zhang, W.; Horoszewski, D.; Decatur, J.; Nuckolls, C. *J. Am. Chem. Soc.* **2003**, *125*, 4870−4873. (n) Wu, Z.-Q.; Jiang, X.-K.; Zhu, S.-Z.; Li, Z.-T. *Org. Lett.* **2004**, *6*, 229−232. (o) Preston, A. J.; Fraenkel, G.; Chow, A.; Gallucci, J. C.; Parquette, J. R. *J. Org. Chem.* **2003**, *68*, 22−26. (p) Gawronski, J.; Gawronska, K.; Grajewski, J.; Kacprzak, K.; Rychlewska, U. *J. Chem. Soc., Chem. Commun.* **2002**, 582−583.

(12) Reviews and lead references to abiotic multiply stranded foldamers: (a) Lehn, J.-M.; Rigault, A.; Siegel, J.; Harrowfield, J.; Chevrier, B.; Moras, D. *Proc. Natl. Acad. Sci. U.S.A.* **1987**, *84*, 2565−2569. (b) Piguet, C.; Bernardinelli, G.; Hopfgartner, G. *Chem. Rev.* **1997**, *97*, 2005−2062. (c) Albrecht, M. *Chem. Rev.* **2001**, *101*, 3457−3498. (d) Berl, V.; Huc, I.; Khoury, R. G.; Krische, M. J.; Lehn, J. M. *Nature* **2000**, *407*, 720−723. (e) Archer, E. A.; Gong, H.; Krische, M. J. *Tetrahedron* **2001**, *57*, 1139−1159. (f) Gong, B. *Synlett* **2001**, *5*, 582−589.

(13) Lead references and reviews of abiotic single-stranded foldamers that bind metals: (a) Prince, R. B.; Okada, T.; Moore, J. S. *Angew. Chem., Int. Ed.* **1999**, *38*, 233−236. (b) Mizutani, T.; Yagi, S.; Morinaga, T.; Nomura, T.; Takagishi, T.; Kitagawa, S.; Ogoshi, H. *J. Am. Chem. Soc.* **1999**, *121*, 754−759. (c) Constable, E. C. *Tetrahedron* **1992**, *48*, 10013−10059. (d) Constable, E. C.; Drew, M. G. B.; Forsyth, G.; Ward, M. D. *J. Chem. Soc., Chem. Commun.* **1988**, 1450−1451. (e) Ho, P. K.-K.; Cheung, K.-K.; Peng, S.-M.; Che, C.-M. *J. Chem. Soc., Dalton Trans.* **1996**, 1411−1417. (f) Kim, H.-J.; Zin, W.-C.; Lee, M. *J. Am. Chem. Soc.* **2004**, *126*, 7009−7014.

(14) The exterior turns of the helical structure described by Moore and co-workers (ref 13a) are templated by each of the silver atoms, whereas the central turn of the structure is controlled by noncovalent interactions.

(15) Dai, Y.; Katz, T. J. *J. Org. Chem.* **1997**, *62*, 1274−1285.

(16) (a) Zhang, H.-C.; Huang, W.-S.; Pu, L. *J. Org. Chem.* **2001**, *66*, 481−487. (b) Pu, L. *Chem. Rev.* **1998**, *98*, 2405−2494.

(17) Tanaka, M.; Fujii, Y.; Okawa, H.; Shinmyozu, T.; Inazu, T. *Chem. Lett.* **1987**, 1673−1674.

Scheme 3

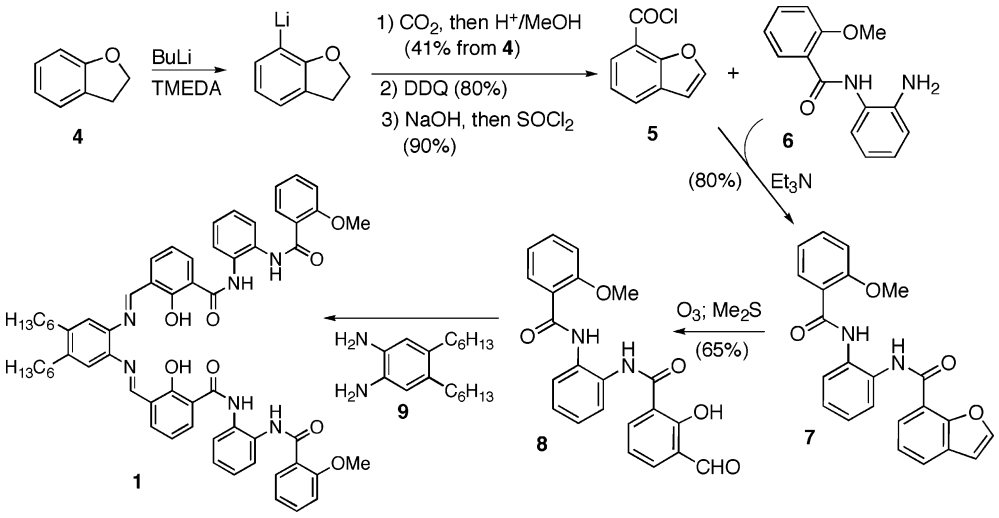

outlined in Figure 2. Our hypothesis was that a stable helix would result for square planar metal complexes of ligand **1** as a result of four six-membered hydrogen bonds between amide donors and phenolic acceptors (Figure 2a). The helical conformer would be further reinforced by a series of aromatic π-stacking interactions between every fourth aromatic ring in the sequence (as depicted in Figure 2b). The core of the secondary structure could be thought of as a chiral analogue of the macrocycle **3**[17] (Figure 2c), which adopts a planar structure with six-membered ring H-bonds.

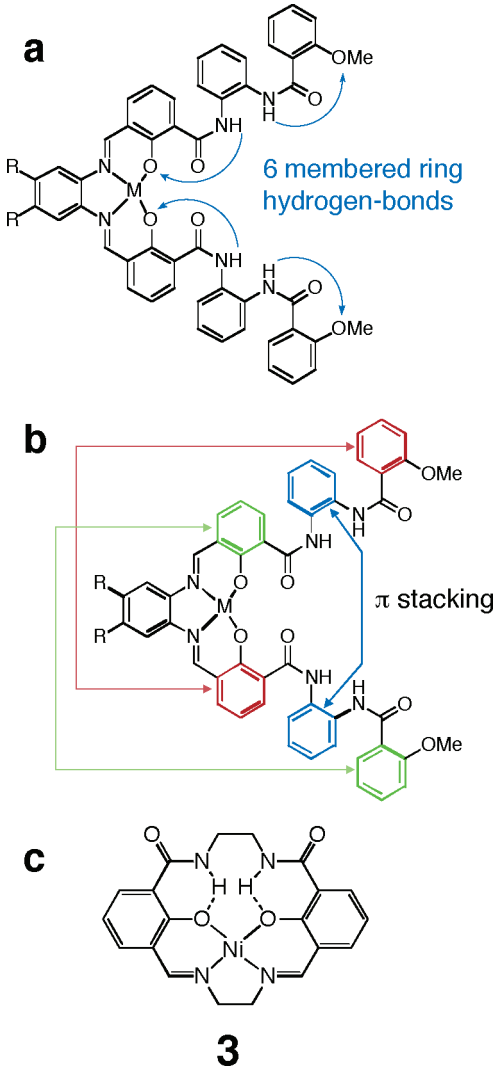

Figure 2. Design of metal-dependent helical foldamers.

Ligand **1** can be synthesized as shown in Scheme 3. Our approach makes use of Stanetty's protocol[18] for making 7-benzofuran carboxylic acid and precedent for preparing salicylaldehydes with amide functionality through ozonolysis of benzofurans.[19] The advantage of this route is that **5** can be prepared in multigram quantities, and that the amide bond-forming reactions are straightforward. Thus, while more expedient syntheses of **1** can be envisioned, the synthesis in Scheme 3 was ideal from a discovery perspective. The metal complexes **2a** and **2b** were prepared in good yields (Scheme 2, 73% for **2a**, 75% for **2b**) by combination of **1** with $Ni(OAc)_2$ and $Cu(OAc)_2$, respectively.

Model Compounds. Before the preparation of **2a** and **2b**, we first prepared the smaller models **11** (Scheme 4) and **14** (displayed in Figure 7). The syntheses mirrored those of **2a** and **2b**. For example, the reaction of *p*-toluidine with **5** and subsequent ozonolysis gave **10**, which condensed with $Ni(OAc)_2$ to give **11**. A similar sequence transforms **13** to **14** (structures displayed in Figure 7). Like the larger analogues **2a** and **2b**, **11** and **14** adopt helical secondary structures, but their metal-free precursors do not. These compounds establish the generality of helical folding for a class of metal complexes. Further, the X-ray structure of ligand **10** provides structural support

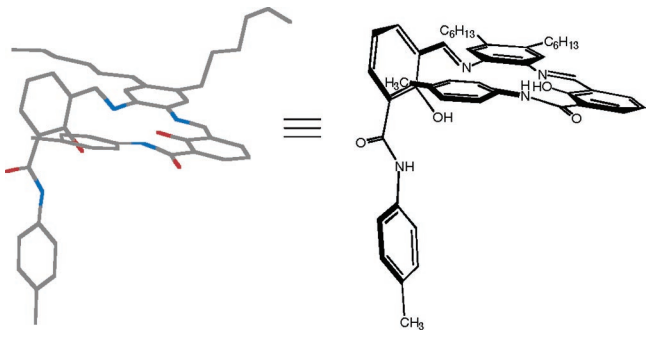

Figure 3. Molecular diagram for ligand **10** prepared in Chem3D using crystallographic coordinates. A thermal ellipsoid plot is available in the Supporting Information.

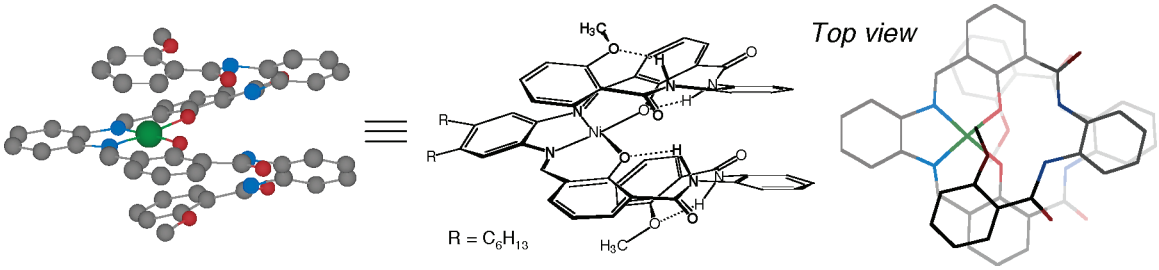

Figure 4. Molecular diagrams for nickel complex **2a** in Chem3D prepared from the crystallographic coordinates. The *n*-hexyl chains have been deleted for clarity of presentation. A thermal ellipsoid plot is available in the Supporting Information.

Scheme 4

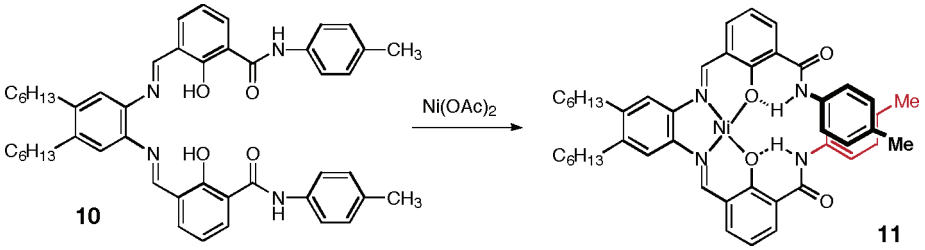

for our claim that such ligands do not fold if the metal is absent. X-ray quality crystals of **10** could be grown directly in the reaction mixture from which it was prepared (EtOH). The structure of **10** is shown in Figure 3. Although we were unable to grow X-ray quality crystals of **11**, solution NMR studies (vide infra) show that it is a helix in solution, whereas the structure of free-ligand **10** is not helical in solution or in the crystal.

Crystallographic and Racemization Studies of 2a and 2b. X-ray diffraction of both **2a** and **2b** revealed nearly identical structures for the two metal complexes of ligand **1**. Two perspectives of the structure of **2a** are displayed in Figure 4, and the structure of **2b** is displayed in Figure 5.

For a foldamer to be useful as a responsive material, it is necessary that its secondary structure be able to form and reform easily. Because we were able to grow large crystals of enantiomerically pure **2a** and **2b**, it was possible to test the stability of those helical molecules toward racemization in solution. Both **2a** and **2b** spontaneously resolve upon crystallization; crystals of **2a** were grown from $CHCl_3/CH_3CN$ and crystals of **2b** from $CHCl_3$/hexanes. Interestingly, a crystal of compound **2a** that was grown from a different solvent system ($MeOH/CHCl_3$) formed racemic crystals in a centrosymmetric space group instead, although the structure of the individual molecules was still helical.

Nonracemic **2a** and **2b** would be expected to possess significant chiroptical properties. As a point of reference, we prepared chiral salen derivative **12** (Figure 6) from **8**, (*R*,*R*)-(−)-*trans*-1,2-cyclohexanediamine, and $Ni(OAc)_2$. Complex **12** has a strong CD spectrum (Figure 6) and a large specific rotation ($[\alpha]^{25}_D$ −730°). We note that the strength of the circular dichroisms for **12** is significantly larger than that of *N*,*N*′-bis(salicylidene)-(*R*,*R*)-cyclohexane-1,2-diaminonickel(II).[20] For example, the bands for **12** that we assign as d−π* charge-transfer transitions[20b] (418 nm, $\Delta\epsilon$ −23; 444 nm, $\Delta\epsilon$ −18) are approximately 3 times larger than those previously reported for *N*,*N*′-bis(salicylidene)-(*R*,*R*)-cyclohexane-1,2-diaminonickel-(II) (413 nm, $\Delta\epsilon$ −8). We submit that the large CD signals provide evidence that the structure of **12** is helical. By analogy, strong circular dichroisms have previously been assigned to the d−π* charge-transfer transitions of polymeric chiral salophens derived from helicenes ($\Delta\epsilon \sim 100$)[15] and binaphthyls ($\Delta\epsilon \sim 45$).[16] The even larger dichroisms for the polymeric materials are partly due to increased conjugation through the phenylene (as opposed to a cyclohexane) and to additional conjugation through the helicenes for the former materials.

To determine the stability of metallofoldamers toward racemization, we chose a large (∼2 mm) crystal of **2a** that we determined to be single by polarized light optical microscopy. From the X-ray diffraction data obtained from an appropriately dimensioned section of the single crystal, it was determined that **2a** crystallized in the noncentrosymmetric space group $P2_12_12_1$ and, therefore, spontaneously resolved. From a refinement of the Flack parameter based on anomalous dispersion effects, the data crystal was 94% enantiomerically pure. The remaining pieces from the original single crystal were then dissolved in CH_2Cl_2 (3.5×10^{-4} M) at 5 °C, and the CD spectrum was recorded. Data acquisition was completed within 5 min of the sample preparation, and no signal could be detected. A similar experiment conducted at room temperature at the polarimeter showed no rotation at the D-line of sodium. The conclusion is that solutions of **2a** racemize quickly at 5 °C, and the implication is that geometrical changes at the metal center are capable of reorganizing the entire secondary structure. When an identical series of experiments were performed with **2b** having a crystal phase isomorphous to that of **2a** and with a refined 99% enantiomeric purity, the conclusion was the same: the helix had racemized at 5 °C before we were able to record a CD spectrum. The implication is that the *thermodynamic* structures of **2a** and **2b** are helical in solution. A useful analogy can be drawn to the helicenes,[21] which also represent a class of thermodynamically helical structures that racemize.

(18) (a) Stanetty, P.; Pürstinger, G. *J. Chem. Res. (M)* **1991**, 78. (b) Stanetty, P.; Koller, H.; Pürstinger, G. *Monatshefte für Chemie* **1990**, *121*, 883−891.
(19) Toyota, E.; Itoh, K.; Sekizaki, H.; Tanizawa, K. *Bioorg. Chem.* **1996**, *24*, 150−158.
(20) (a) Downing, R. S.; Urbach, F. L. *J. Am. Chem. Soc.* **1970**, *92*, 5861−5865. (b) Bosnich, B. *J. Am. Chem. Soc.* **1968**, *90*, 627−632. (c) Costes, J. P.; Dominguez-Vera, J. M.; Laurent, J. P. *Polyhedron* **1995**, *14*, 2179−2187.

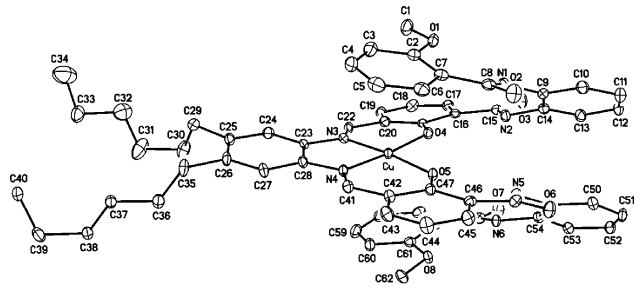

Figure 5. Molecular diagram of copper complex **2b** depicted with ellipsoids at 30% probability. Solvent molecules and hydrogen atoms are omitted for clarity.

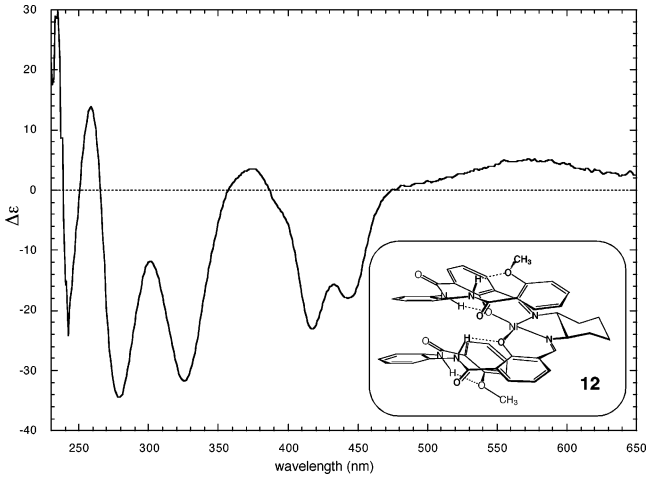

Figure 6. CD spectrum of **12** (2.2×10^{-4} M in CH_2Cl_2).

Solution NMR Studies: Chemical Shift Anisotropy as a Measure of Helicity. NMR studies evidence that Ni complex **2a** and smaller analogues **11** and **14** are helical in solution, whereas their free ligands are not. One way that this could be demonstrated was by directly comparing the ^{1}H chemical shifts of the aromatic protons of the metal complexes to free ligands. For example, if Ni complex **14** were to adopt a helical conformation, then it would be expected that hydrogens of the terminal tolyl rings would resonate at a substantially higher field than the analogous protons on reference compound **13**. Chemical shift anisotropy[22] of this type is well-known for helical aromatic molecules,[21] and it has been used to provide evidence for the helical solution structure of several types of peptidomimetic foldamers, including oligoanthranilimides[11d] and oligo-*m*-phenyleneethynylenes.[13a] Indeed, chemical shift analysis does suggest that the solution structures of Ni complexes **11** and **14** are helical, as the protons of the tolyl group resonate at substantially higher field than those of **13**. For **14**, The $\Delta\delta$ values are 0.57 and 0.42 ppm for the aromatic resonances, and $\Delta\delta =$ 0.16 ppm for the methyl resonances. In comparison, the corresponding hydrogens on the salicyl rings of **13** and **14** have chemical shifts that nearly coincide. Thus, the large changes in chemical shift must be attributed to the underlying ring currents rather than to an electronic effect upon metal binding since metal coordination should perturb the electronics of the salicyl hydrogens more strongly than those of the tolyl. The aromatic hydrogens and methyls on the tolyl group of nonracemic Ni

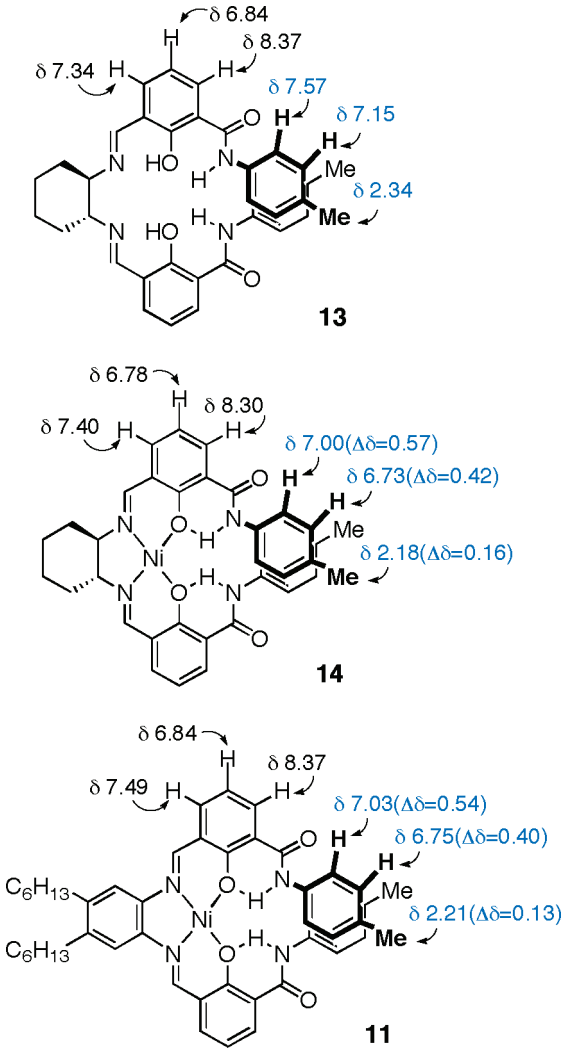

Figure 7. Chemical shift anisotropy as a measure of helicity.

complex **11** have similar chemical shifts to **14** and resonate at high field when compared to the corresponding hydrogens of **13**. The $\Delta\delta$ values are 0.54 and 0.40 ppm for the aromatic hydrogens and 0.13 for the methyl groups. Again, the perturbation of the salicyl aromatic hydrogens is minor.

NMR spectral studies on the larger structure **2a** strongly suggest that the solution structure is also helical. This was demonstrated in part by comparing the ^{1}H NMR spectra of **2a** with reference compounds **6**, **7**, **8**, and **11**. Unambiguous chemical shift assignments for each of the 14 different hydrogens and 22 different carbons of the core structure of **2a** were made by an extensive series of NMR studies (HMBC, HSQC, and COSY). Similarly, rigorous assignments were made for each of the model compounds **6**, **7**, **8**, and **11**. Nine hydrogens in **2a** were found to resonate at significantly higher field when compared to the reference compounds (Figure 8). Anisotropic effects are observed both at the core and at the ends of the structure. The hydrogens on the terminal methoxy groups of **2a** are shifted upfield by ~0.6 ppm in comparison to **8**, and the hydrogens bound to the imines (H21) are shifted upfield by 0.43 ppm relative to **11**. A table is provided in the Supporting Information that compares all of ^{1}H NMR chemical shifts for **2a** and **6**−**8** (those for **11** are in Figure 8) and supports the assertion that the solution structure of **2a** is a helix.

(21) Laarhoven, W. H.; Prinsen, W. J. C. *Top. Curr. Chem.* **1984**, *125*, 63−130.
(22) Abraham, R. J.; Fell, S. C. M.; Smith, K. M. *Org. Magn. Reson.* **1977**, *9*, 367 and references therein.

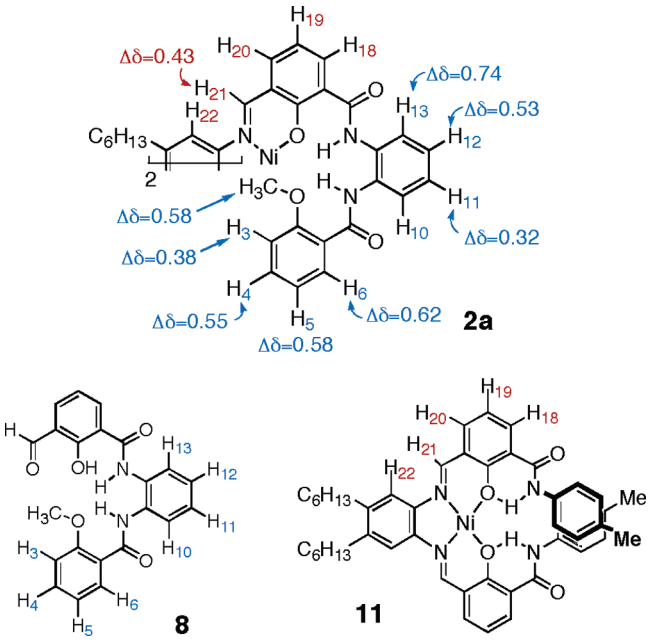

Figure 8. Comparison of the ^{1}H NMR chemical shifts of **2a** with **8** or **11**. The chemical shifts of hydrogens with blue labels were compared to **8**, and hydrogens with red labels were compared to **11**. The $\Delta\delta$ values refer to upfield chemical shifts. H10, H18−H20, and H22 did not show significant differences when compared to these standards. A table with all of the chemical shift data is displayed in the Supporting Information.

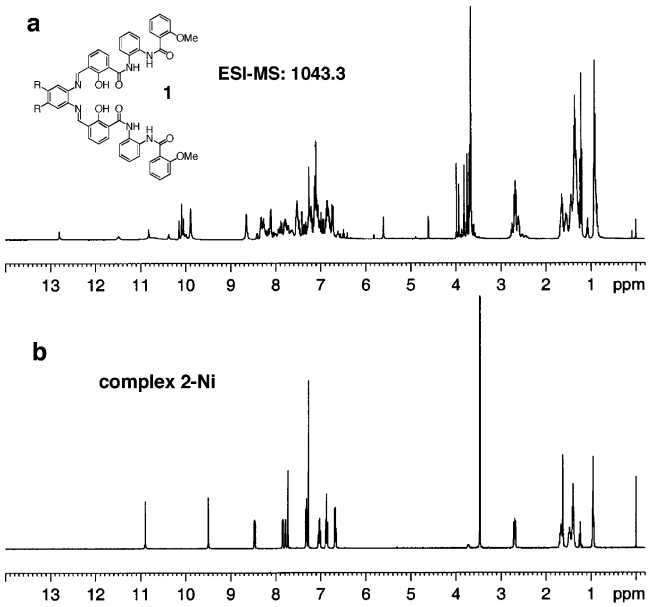

Figure 9. (a) ^{1}H NMR spectrum ($CDCl_3$) of ligand **1** (>70% pure). (b) ^{1}H NMR spectrum of **2a** ($CDCl_3$). The complexity of the NMR spectrum of **1** is attributed to intermolecular aggregation.

It was not possible to directly compare free-ligand **1** with **2a** because **1** has an extremely complex ^{1}H NMR spectrum in $CDCl_3$ or CD_2Cl_2 (the solvents in which extensive NMR characterization was performed for **2a**). The ^{1}H NMR spectrum of **1** provides a stark contrast to the crisp spectrum of **2a** (Figure 9). Despite the complexity of the NMR spectrum, the formation of the ligand was confirmed by the observation of a prominent parent peak (1043.3 = M + Na) by ESI MS. It was considered that the complex NMR spectrum is observed for **1** because it adopts several secondary structures that do not interconvert on the NMR time scale. If this interpretation were correct, then it would be expected that upon heating that the ^{1}H NMR spectrum of **1** might coalesce. We heated a solution of **1** in DMSO-d_6 to 100 °C and observed only minor changes in the ^{1}H NMR spectrum. Optical rotation and circular dichroism experiments (vide supra) have shown that complex **2a** racemizes quickly in solution at 5 °C, and in this context, it is difficult to rationalize why the free ligand would adopt secondary structures with such unusual stability. A more likely explanation is that the free-ligand **1**—rich in both H-bond donors and acceptors—forms an aggregate in nonpolar solvents. Consistent with this interpretation, the polar solvent DMF-d_8 disrupts the aggregate. The ^{1}H NMR spectrum in that solvent shows ≥70% of a single compound that we assign as monomeric **1**.

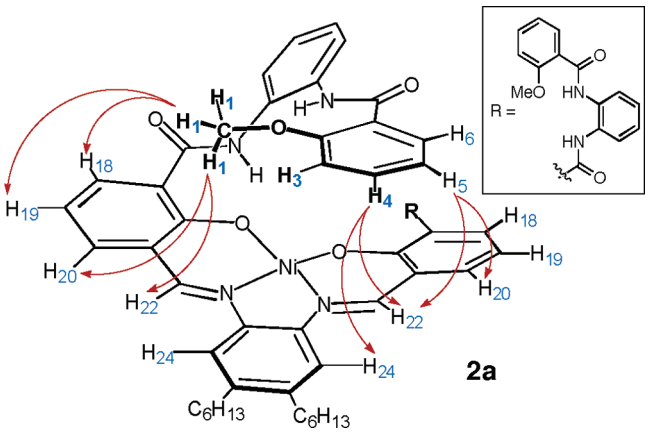

Figure 10. Selected trans-helix NOEs that were observed for **2a**.

NOESY Studies of 2a. That Ni complex **2a** adopts a helical structure in solution is further supported by the phase sensitive NOESY[23] spectra, which show nuclear Overhauser effects between the protons on the terminal anisoyl groups and those on the internal salophen. The observed trans-helix NOE signals are shown in Figure 10. As expected for a molecule of this size, the cross-peaks in the NOESY spectra have the opposite sign with respect to the diagonal—an indication that the cross-peaks arise from positive NOE enhancements. The cross-peaks (H3−H22, H4−H22, H4−H24, H5−H20, H5−H22, H6−H18, H6−H19, and H6−H20) shown in Figure 11 qualitatively confirm the close proximities between terminal anisoyl and salophen protons. The cross-peaks (OCH_3−H18, OCH_3−H19, OCH_3−H20, OCH_3−H22, and OCH_3−H24) between methoxy protons on the anisoyl group and salophen protons further support the assignment of a helical structure in solution.

Conformational analysis using NOE can be especially challenging[24] for small molecules. External relaxations (often termed "leakages") introduce additional relaxation mechanisms that may interfere with the NOE measurements. Leakage is particularly problematic for small molecules, even when precautionary measures (choosing shorter mixing times, carefully degassing the solution) are taken. The high conformational flexibility of small molecules often makes estimation of the internuclear distances impossible. An implication for foldamers is that the observation of NOE signals can be taken as an indicator of a stable secondary structure.

(23) Macura, S.; Huang, Y.; Suter, D.; Ernst, D. D. *J. Magn. Reson.* **1981**, *43*, 259−281.
(24) Claridge, T. D. W. *High-Resolution NMR Techniques in Organic Chemistry*; Pergamon: Amsterdam, 1999.

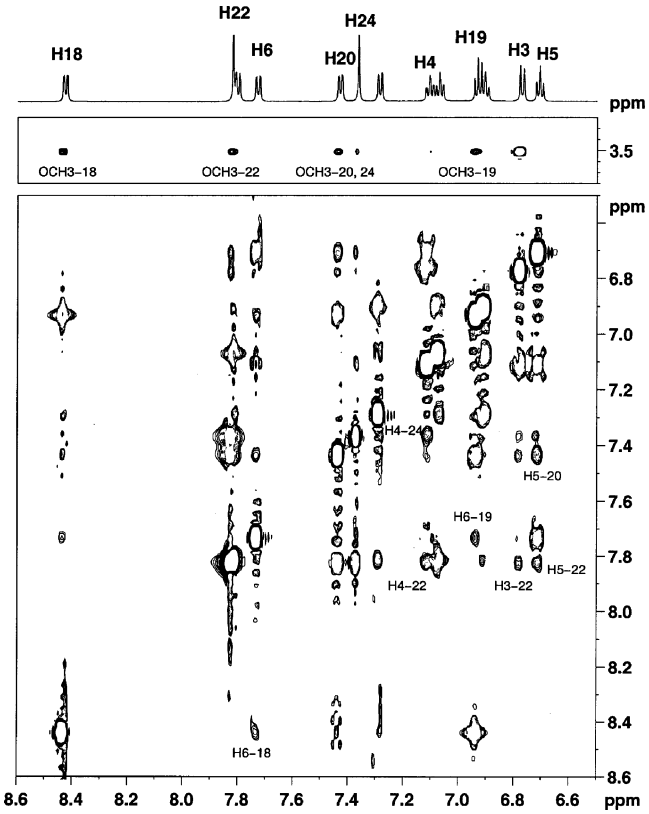

Figure 11. NOESY spectrum of **2a**.

Quantitative NOE measurements were conducted on **2a** using the intensity ratio method,[25] which extracts internuclear distances from the intensity ratio of cross and diagonal peaks from a single NOESY spectrum. The intensity ratio method is experimentally much more straightforward than the "NOE build-up" method,[26] which requires a series of NOESY spectral acquisitions as a function of mixing time. Both methods have been shown to be in excellent agreement for the evaluation of distances in small molecules.[25e] The interproton separation, r, is expressed in terms of the molecular correlation time, τ_c, and the mixing time, τ_{mix}, as follows (eq 1):[25d,e]

$$r = \left\{ \frac{0.2\,\gamma^4\hbar^2(\mu_0/4\pi)^2\,\tau_{mix}}{\ln\left[\frac{I_{aa}+I_{ab}}{I_{aa}-I_{ab}}\right]} \left(\frac{6\tau_c}{1+4\omega^2\tau_c^2}\right) - \tau_c \right\}^{1/6} \quad (1)$$

I_{aa} and I_{ab} are intensities of diagonal and cross-peaks, respectively, and ω is the proton Larmor frequency. Using eq 1, the molecular correlation time, τ_c, of Ni complex **2a** is calculated to be 5.4×10^{-11} s from an interproton distance of 2.8 Å for ortho-substituted benzene protons[24] H18−H19 (see Figure 10 for atom labels). The experimental mixing time of 0.8 s and the NOE cross and diagonal peak intensities of H18 and H19 were used in these calculations. If the assumption[27] is made that the molecular tumbling is isotropic and interproton vectors possess the same correlation time, the interproton distances of the terminal anisoyl protons and those on the internal salophen can be calculated from a single NOESY spectrum with a correlation time of 5.4×10^{-11} s. The assumption should be valid if **2a** adopts a stable helix. The interproton separations listed in the table are the pairs between the terminal anisoyl aromatic or methoxy protons and the internal salophen protons. The NOE interproton distances are listed in Table 1 and are compared to the distances obtained from the X-ray crystallographic studies described in the previous section. In general, the distances as measured by X-ray are in close agreement to those measured by the NOE experiment. In accord with the conclusion from the NMR anisotropy studies, the results of the NOE analysis strongly suggest that the helical conformation of **2a** in crystal is preserved in solution.

Table 1. Internuclear Distances of Ni Complex **2a** from NOESY and X-ray Crystallography

proton pair	distance (NOE)[a] Å	distance (X-ray)[c] Å
H3−H22	4.60	4.45
H4−H22	3.94	3.82
H4−H24	4.10	4.64
H5−H20	3.98	3.43
H5−H22	4.38	4.17
H6−H18	4.55	4.11
H6−H19	4.52	3.94
H6−H20	4.28	3.80
OCH_3−H18	5.08[b]	4.66, 6.24, 5.76 (5.25)[d]
OCH_3−H19	5.21[b]	5.15, 6.55, 5.92 (5.67)[d]
OCH_3−H20	4.17[b]	4.71, 4.73, 5.77 (4.93)[d]
OCH_3−H22	4.95[b]	4.30, 4.95, 3.66 (4.08)[d]
OCH_3−H24	5.10[b]	6.65, 5.78, 4.58 (5.12)[d]

[a] Distances obtained using the intensity ratio method or eq 1; an estimated error of 0.3 Å is expected in case of a 50% inaccuracy[25d] of the intensity ratio. [b] The cross-peak intensity of methoxy protons was divided by 3 since diagonal peaks of H18−H24 were used in the calculations. [c] X-ray distances are obtained by simply adding hydrogen in the X-ray structures, realizing that these distances merely serve as the benchmarks to validate NOE distances. [d] The rapid internal rotation of the methyl group, on the NMR time scale, dictates that only the time average of interproton distance is meaningful. The numbers in parentheses are calculated from the X-ray distance of these protons based on $\langle r^{-6}\rangle^{-1/6}$ and represent the mean values of three proton positions. This mean value is heavily weighted on the shorter distances because of a r^{-6} dependence of the NOE distances.

Electrochemical Studies. Cyclic voltammograms (CV) of **2b** in THF and CH_2Cl_2 are displayed in Figure 12. In THF, the CV shows a single, reversible one-electron transfer at $E_{1/2} = -0.63$ V that was unaltered after three repeated cycles. A similar CV was recorded in CH_2Cl_2 with $E_{1/2} = -0.75$ V. After correcting for the proportional shift of the ferrocenium/ferrocene couple (0.801 V in THF versus 0.701 in CH_2Cl_2.), a small (20 mV) cathodic shift is observed when the solvent is changed from THF to CH_2Cl_2. These CVs are indicative of metal-centered Cu(II)/Cu(I) redox events for a Cu−salophen derivative.[28] The shift to a more positive potential as compared to that of unsubstituted Cu−salophen ($E_{1/2} = -1.11$ V) is an expected consequence of substituting the salophen nucleus by

(25) (a) Bodenhausen, G.; Ernst, R. R. *J. Am. Chem. Soc.* **1982**, *104*, 1304−1309. (b) Macura, S.; Farmer, B. T.; Brown, L. R. *J. Magn. Reson.* **1986**, *70*, 493−499. (c) Esposito, G.; Carver, J. A.; Boyd, J.; Campbell, I. D. *Biochemistry* **1987**, *26*, 1043−1050. (d) Esposito, G.; Pastore, A. *J. Magn. Reson.* **1988**, *76*, 331−336. (e) Reggelin, M.; Hoffmann, H.; Köck, M.; Mierke, D. F. *J. Am. Chem. Soc.* **1992**, *114*, 3272−3277.
(26) Kumar, A.; Wagner, G.; Ernst, R. R.; Würhrich, K. *J. Am. Chem. Soc.* **1981**, *103*, 3654−3658.
(27) (a) Keepers, J. W.; James, T. L. *J. Magn. Reson.* **1984**, *57*, 404−426. (b) Andersen, N. H.; Eaton, H. L.; Lai, X. *Magn. Reson. Chem.* **1989**, *27*, 515−528.
(28) (a) Patterson, G. S.; Holm, R. H. *Bioinorg. Chem.* **1975**, *4*, 257−275. (b) Rohrbach, D. F.; Heineman, W. R.; Deutsch, E. *Inorg. Chem.* **1979**, *18*, 2536−2542. (c) Doine, H.; Stephens, F. F.; Cannon, R. D. *Inorg. Chim. Acta* **1983**, *75*, 155−157. (d) Zanello, P.; Cinquantini, A. *Transition Met. Chem.* **1985**, *10*, 370−374.

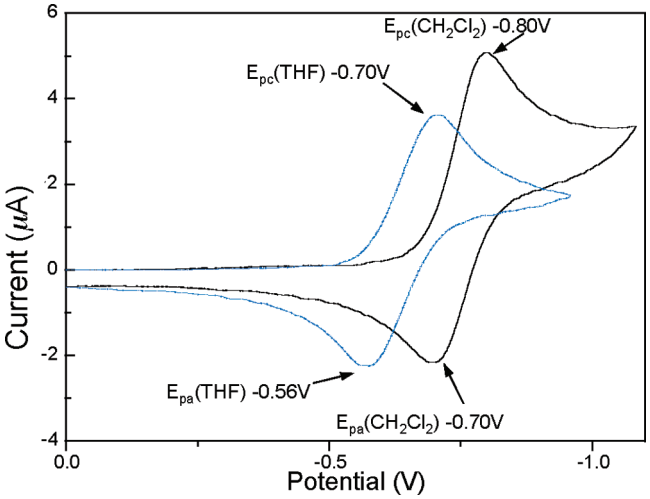

Figure 12. Cyclic voltammograms of **2b** (1×10^{-3} M) with $^{n}Bu_4NPF_6$ (0.1 M) as supporting electrolyte. A platinum electrode was used as working electrode, together with a platinum wire auxiliary electrode. The reference Ag/Ag+ electrode is filled with the supporting electrolyte solution (0.1 M $^{n}Bu_4NPF_6$). Ferrocene was used as an internal standard (1×10^{-3} M), and potentials were rescaled to E_0(Fc/Fc+) = 0.801 V versus NHE (THF) and to E_0(Fc/Fc+) = 0.701 V versus NHE (CH_2Cl_2).

electron-withdrawing groups that are in conjugation with the phenolic oxygens.[29] In contrast to the reversible behavior observed in THF or CH_2Cl_2, quasireversible behavior was observed when the CV of **2b** was measured in CH_3CN (Figure 13). Thus, while a single peak ($E_{pc} = -0.75$ V) was observed during the cathodic sweep, two waves ($E_{pa} = -0.60$ and -0.16 V) were observed during the anodic sweep. With the $E_{1/2}$ of ferrocenium/ferrocene as the reference point, the E_{pc} for **2b** in acetonitrile is anodically shifted by 80 mV compared to the E_{pc} of **2b** in THF or CH_2Cl_2. The CV was also measured for a solution of **2b** in THF containing 5% *N*,*N*-4-(dimethylamino)-pyridine (DMAP), and irreversible behavior was noted. Thus, while the peak observed during the cathodic sweep was similar to that observed in pure THF, a large shift (from -0.70 in THF to -0.26 V in THF/DMAP) was observed during the anodic sweep.

While a tetrahedral geometry is most usual for tetracoordinate Cu(I), the rigidity of the salophen ligand precludes tetrahedral coordination. In the late 1970s, Gagné characterized and studied a number of complexes of Cu(I) with tetradentate ligands that enforce near-planar coordination[30] and found that Cu(I) complexes of such ligands sometimes adopt distorted square planar geometries.[30d,e] Alternatively, Cu(I) complexes of this type can form five-coordinate, square pyramidal structures (e.g., crystallographically characterized **15**,[30] Figure 14) when they are generated in the presence of monodentate ligands, such as carbon monoxide, isonitriles, phosphates, phosphines, *N*-methylimidazole, or acetonitrile.[30] Although binding of external ligands to Cu(I)−salen or Cu(I)−salophen has not been investigated extensively, the binding of carbon monoxide to these complexes was studied and found to give a square pyramidal complex,[30a] and apical solvent coordination has been suggested for electrochemically generated Cu(I)−salen complexes in DMF.[31] Apical coordination of solvent is also observed in crystallographically characterized Zn(II)−salen complexes (e.g., **16**,[32] Figure 14), which are expected to be isostructural to their Cu(I) analogues.

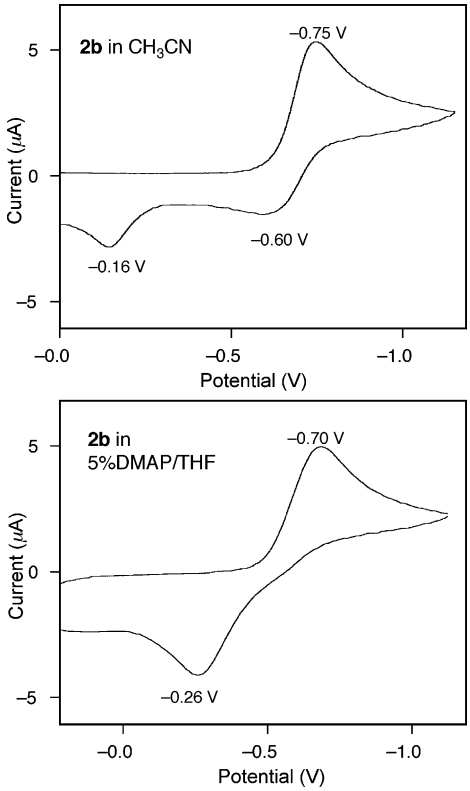

Figure 13. Cyclic voltammograms of **2b** (1×10^{-3} M) in acetonitrile (top) and in 5% DMAP/THF (bottom). $^{n}Bu_4NPF_6$ (0.1 M) was the supporting electrolyte. A platinum electrode was used as working electrode, together with a platinum wire auxiliary electrode. The reference Ag/Ag+ electrode is filled with the supporting electrolyte solution (0.1 M $^{n}Bu_4NPF_6$). Ferrocene was used as an internal standard (1×10^{-3} M), and potentials were rescaled to E_0(Fc/Fc+) = 0.801 V versus NHE (THF) and to E_0(Fc/Fc+) = 0.651 V versus NHE (CH_3CN).

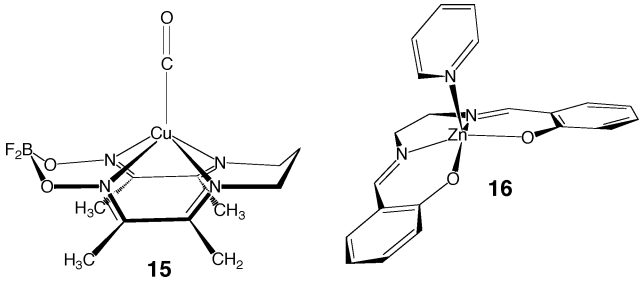

Figure 14. Square pyramidal complexes of Cu(I) and Zn(II) from tetradentate, macrocyclic ligands.

We propose that Cu(I)−**2b** is tetracoordinate when generated electrochemically in CH_2Cl_2. This interpretation is consistent with the reversible nature of the CV data, the expectation that CH_2Cl_2 would be a poor ligand, and the small solvent effect upon changing to THF. Solvent coordination cannot be com-

(29) Zolezzi, S.; Spodine, E.; Decinti, A. *Polyhedron* **2002**, *21*, 55−59.
(30) (a) Gagné, R. R.; Allison, J. L.; Ingle, D. M. *Inorg. Chem.* **1979**, *18*, 2767−2774. (b) Gagné, R. R.; Allison, J. L.; Gall, R. S.; Koval, C. A. *J. Am. Chem. Soc.* **1977**, *99*, 7170−7178. (c) Gagné, R. R. *J. Am. Chem. Soc.* **1976**, *98*, 6709−6710. (d) Gagné, R. R.; Koval, C. A.; Smith, T. J. *J. Am. Chem. Soc.* **1977**, *99*, 8367−8368. (e) Gagné, R. R.; Allison, J. L.; Lisensky, G. C. *Inorg. Chem.* **1978**, *17*, 3563−3571.
(31) The role of the solvent as a ligand in electrochemical reduction of Cu−salophen has been pointed out by Deutsch,[28b] who compared the reductions of Cu(II) and Co(II) Schiff base complexes in DMF and noted the "similar dependencies of the Cu(I)/C(II) and Co(I)/Co(II) couples on equatorial ligand structure (with the common axial ligand DMF)".
(32) Reglinski, J.; Morris, S.; Stevenson, D. E. *Polyhedron* **2002**, *21*, 2175−2182.

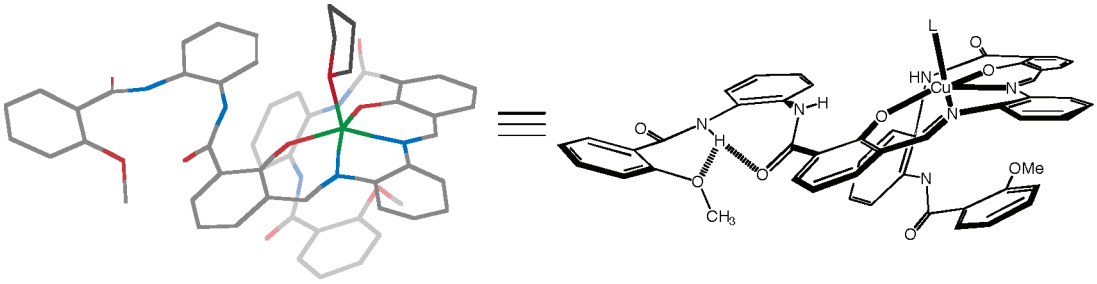

Figure 15. Calculated (AM1) low energy conformer of a square pyramidal complex of **2b**. The model implies that apical coordination of any ligand (i.e., CH_3CN, DMAP, or THF) will disrupt folding on that face. The apical ligand for the calculation is THF.

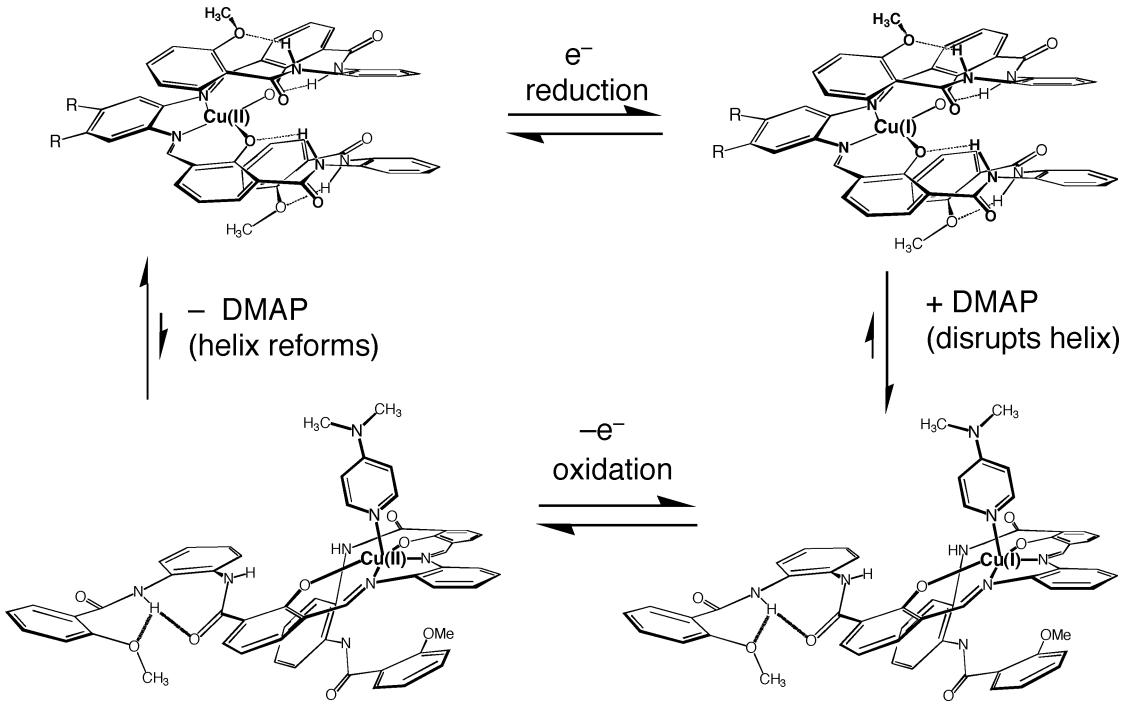

Figure 16. Model for quasireversible redox behavior of **2b** in the presence of the external ligand 4-(dimethylamino)pyridine. Ligand association occurs after electrochemical reduction and disrupts the helical secondary structure of the complex. Electrochemical oxidation and subsequent ligand dissociation regenerate the helical Cu(II) complex. Quasireversible behavior is also observed when CH_3CN is the external ligand.

pletely ruled out for THF, but the reversible nature of the CV and the small magnitude of the anodic shift relative to CH_2Cl_2 imply that the binding constant for THF is small. However, the effect of switching solvent to acetonitrile is significant and provides strong evidence that acetonitrile binds after the electrochemical reduction step. We propose that the resulting complex is pentacoordinate and structurally analogous to **15** and **16**. During the anodic sweep, more than one mechanism is in operation. We attribute the peak at −0.60 V to solvent dissociation prior to oxidation, whereas the peak at −0.16 V is assigned to the electrochemical oxidation of the acetonitrile complex. For the latter mechanism, dissociation of acetonitrile should occur rapidly upon oxidation; we find no change in the UV−vis absorption spectrum of Cu(II)−**2b** when the solvent is changed from THF to THF/acetonitrile. In 5% DMAP/THF, the CV is irreversible. Again, we propose five-coordinate binding in analogy to **15** and **16**, and that the binding occurs after the electrochemical reduction. We attribute the peak at −0.26 mV to the electrochemical oxidation of the pentacoordinate complex; dissociation of DMAP does not take place prior to oxidation. As is the case for the acetonitrile complex, we expect that ligand dissociation is rapid upon reoxidation; we find no difference between the UV−vis absorption spectrum of Cu(II)−**2b** in pure THF versus 5% DMAP/THF.

Computational Studies. Apical coordination to **2b** in a manner analogous to that of **15** and **16** would completely block one face of the salophen and, by necessity, disrupt the helix on that face. Because the electrochemical experiments provide direct evidence for ligand binding, they also provide evidence for reversible helix folding and unfolding. To gain insight into the structure of the pentacoordinate species, we modeled the structure of the Cu(I) form of **2b** with THF as an apical ligand. The core structure of the salophen and the oxygen of the THF were held fixed during the calculations, and the metal atom was replaced by a stationary "dummy" atom to hold the place of copper. Calculations were conducted at the semiempirical (AM1) level. Some of the starting geometries for the semiempirical calculations were manually selected, logical starting points that could maximize noncovalent interactions. We also selected starting points for the AM1 calculation by taking the lowest energy structures from a molecular mechanics (MM3) Monte Carlo multiple minimum search. All of the local minima that we identified from the AM1 calculations have structures in which helicity is disrupted on the face to which the apical ligand

is bound. In the lowest energy configuration that we calculated (Figure 15), the top face of the molecule is extended and stabilized by a new intramolecular hydrogen bond between the carbonyl of the internal amide and the N−H of the external amide. While THF was the apical ligand for this computational study, it is apparent that apical binding of any ligand (e.g., DMAP or acetonitrile) would disrupt the helix on that face. Thus, the redox behavior of metallofoldamer **2b** can be correlated to a dramatic change in secondary structure in coordinating environments. Figure 16 summarizes the structural reorganization that takes place upon redox cycling. Future studies will be directed toward altering materials' properties (e.g., NLO, liquid crystallinity) in response to reversible perturbations of foldamer structure.

Conclusions

In summary, we have designed and synthesized nonbiological molecules based on salophen and salen ligands that can fold into single-stranded helices in the presence of either Ni(II) or Cu(II). That the structures are folded is strongly supported by X-ray diffraction and NMR studies. Metal coordination is required for folding, as these same techniques show that the free ligands do not adopt helical structures. Two of the racemic metallofoldamers spontaneously resolved during crystallization. CD spectroscopy and optical rotation show that both molecules racemize quickly at 5 °C, showing that the secondary structures can reorganize easily and can, therefore, provide the basis for responsive materials. Electrochemical experiments show that a structural reorganization occurs upon metal-centered reduction of a Cu(II)-containing foldamer. When the reduction is carried out in the presence of coordinating ligands, it is proposed that apical binding of those ligands gives square pyramidal complexes. Semiempirical (AM1) calculations support that the helical structure would be disrupted by the reduction to Cu(I) with concomitant reorganization to a square pyramidal complex.

Acknowledgment. The University of Delaware is thanked for financial support of this work. F.Z. is grateful for support received through the competitive University Graduate Fellowship program at UD. We thank Charles Riordan (UD) and Bill Dougherty (UD) for assistance in obtaining and interpreting CV data, and Olga Dmitrenko for assistance with calculations at the AM1 level.

Supporting Information Available: A full experimental description of the preparation and characterization of all new compounds is described. ^{1}H NMR and ^{13}C NMR spectra are displayed for all new compounds. A table compares the chemical shifts of **2a**, **8**, **7**, and **6** to provide a measure of helicity of **2a**. COSY, HSQC, and HMBC data are provided for compounds **6**, **7**, **8**, **2a**, and **11**. HSQC and HMBC data are provided for compound **12**. The ESI MS spectrum of crude **1** is displayed. The CV of **2b** after four repeated cycles is displayed. UV−vis spectra are displayed for compounds **2a**, **2b**, **11**, **12**, and **14**. The CD spectrum of **14** is displayed. X-ray crystallographic data are provided for compounds **2a**, **2b**, and **10**. Also displayed are photographs of crystals of **2a** and **2b** with transmitted light and under cross-polarized transmitted light. This material is available free of charge via the Internet at http://pubs.acs.org.

JA050886C